High-k, ultrastretchable self-enclosed ionic liquid-elastomer composites for soft robotics and flexible electronics

Ankit; Tiwari, Naveen; Ho, Fanny; Krisnadi, Febby; Kulkarni, Mohit Rameshchandra; Nguyen, Linh Lan; Koh, Adrian Soo Jin; Mathews, Nripan

2020

Ankit, Tiwari, N., Ho, F., Krisnadi, F., Kulkarni, M. R., Nguyen, L. L., Koh, A. S. J. & Mathews, N. (2020). High-k, ultrastretchable self-enclosed ionic liquid-elastomer composites for soft robotics and flexible electronics. ACS Applied Materials and Interfaces, 12(33), 37561-37570. https://dx.doi.org/10.1021/acsami.0c08754

https://hdl.handle.net/10356/152973

https://doi.org/10.1021/acsami.0c08754

High-k, Ultra-Stretchable Self-Enclosed Ionic Liquid-Elastomer Composites for Soft Robotics and Flexible Electronics

*Ankit,[1] Naveen Tiwari,[1] Fanny Ho,[1] Febby Krisnadi,[1] Mohit Rameshchandra Kulkarni,[1] Linh Lan Nguyen,[2] Soo Jin Adrian Koh,[3] Nripan Mathews[1,4]**

[1] School of Materials Science and Engineering, Nanyang Technological University, Singapore 639798.

[2] School of Physical and Mathematical Sciences, Nanyang Technological University, Singapore 637371.

[3] Department of Mechanical Engineering, National University of Singapore, Singapore 117575.

[4] Energy Research Institute @ NTU (ERI@N), Nanyang Technological University, Singapore 637553.

KEYWORDS: soft actuators, self-contained liquid-filler polymer composite, dielectric elastomers, ionic liquids, high dielectric composites.

ABSTRACT

Soft robotics focuses on mimicking natural systems to produce dexterous motion. Dielectric elastomer actuators (DEAs) are an attractive option due to their large strains, high efficiencies, lightweight design and integrability but require high electric fields. Conventional approaches to improve DEA performance by incorporating solid fillers in the polymer matrices can increase the dielectric constant, but to the detriment of mechanical properties. In the present

work, we draw inspiration from soft and deformable human skin, enabled by its unique structure which consists of fluid filled membrane, to create self-enclosed liquid filler (SELF)-polymer composites by mixing an ionic liquid into elastomeric matrix. Unlike hydrogels and ionogels, the SELF-polymer composites are made from immiscible liquid fillers, selected based on interfacial interaction with the elastomer matrix, and exist as dispersed globular phases. This combination of structure and filler selection unlocks synergetic improvements in electro-mechanical properties – doubling of dielectric constant, 100 times decrease in Young's modulus and ~5 times increase in stretchability. These composites show superior thermal stability to volatile losses, combined with excellent transparency. These ultra-soft high-k composites enable significant improvement in actuation performance of DEAs – longitudinal strain (5 times) and areal strain (8 times) – at low applied nominal electric fields (4V/μm). They also enable high-sensitivity capacitive pressure sensors without the need of miniaturization and microstructuring. This class of self-enclosed ionic liquid polymer composites could impact the areas of soft robotics, shape morphing, flexible electronics and optoelectronics.

INTRODUCTION

Traditional robots fabricated from rigid components have excelled at performing monotonous, repetitive tasks with high accuracy and precision in controlled environments making them suitable for industrial automation. However, the limited degrees of freedom, finite adaptability and mismatch in mechanical moduli make them unsuitable for human interaction. Soft robots aim to bridge this gap, allowing for a continuously deformable structure combining programmable actuation with biological compliance[1]. They have demonstrated the ability to manoeuvre in constrained spaces, been utilized as artificial muscles[2-5], versatile soft grippers[6], enabled autonomous actuation[7-8], and have even found applications in optics[9]. The technology that powers most of today's soft robotics – Pneumatic actuators (utilizing pressurized air) have

large actuation forces, strokes as well as complex movements achieved by embedded channels. However they have inadequate integrability, low efficiency, poor control requiring bulky compressors which compromises portability[2].

In contrast, electrically powered soft actuators made of elastomers are known for their high efficiencies, light-weight design and superior structural compliance[10-11]. Dielectric elastomer actuators (DEAs) are compliant capacitors with an elastomeric layer sandwiched between electrodes where voltage application triggers Maxwell Stresses which result in actuation (**Figure S1**)[10-11]. The integrability and versatility of DEAs have allowed them to be utilized in applications such as thin film speakers[12], haptic surfaces[10, 13], optics[9, 14] and biomimetic fish robots[15], as well as artificial muscles[2-3] and soft grippers[6]. They have demonstrated high energy densities (0.5–19.8J/kg) and significant actuation performance (2.5–70% actuation strain)[3]. However, these demonstrations still require very high voltages (3.5–13kV) corresponding to high electric fields (30–100V/μm)[3], attributable to the properties of the polymeric acrylates and silicones, which comprise the active elastomeric layer. Such high electric fields required for actuation originate from intrinsic material properties like Young's moduli (0.1 – 1MPa) and dielectric constants (2.8 – 4.8) of the aforementioned polymeric systems.[16] Attempts to reduce Young's modulus through plasticizers and chemical modification have resulted in modest actuation improvements while causing undesirable changes in the viscoelastic properties and volatility.[16-17] Strategies to improve dielectric constants by addition of conductive and high-k ceramic fillers, as well as chemical modification of the polymer backbone, have been accompanied with reliability issues and increased mechanical stiffness (in some cases leading to twenty-fold increase in Young's modulus).[16, 18-19] Thus, conventional approaches focus on improving upon either of the material properties and miss out on bringing synergetic improvements..

In order to break this deadlock, we look to nature for inspiration. Biological materials such as human skin and muscles are solid matrices with distributed liquid phases, and the observed macroscopic mechanical properties like stretchability and stiffness are due to its components, structural organization and mutual interactions between the constituents[20-21]. The human skin (epidermis) has a layered compositional structure **Figure 1**a [22] with varying concentration of fluids amongst them, leading not only to different functionalities but different mechanical properties as well[20]. Stratum Granulosum (**Figure 1**a, Right) has nearly 70% water content and exists similar to a gel-like phase, compared to 15–30% water content in Stratum Corneum[20], which is the outermost layer of the skin. The amount of water content has been correlated to the stiffness and the stretchability of the skin.[20] Hydrogels attempt to mimic the softness of biological materials and consist of cross-linked polymer networks and an aqueous phase[23] incorporated within the polymer network. However, hydrogels undergo significant volume changes caused by the removal of water from the network [24], drastically changing the mechanical properties. In contrast, fluids exist as encapsulated phases in biological materials and flow into any form that the cellular membranes can tolerate, enabling softness and stretchability[20]. A recent approach aims to mimic this structure and fabricate functional composites with liquid fillers rather than solid fillers.[5, 25] However, these approaches have been focused on increasing the dielectric constant and have not managed to imbibe the composites with mechanical softness. Hence, to mitigate issues with conventional composite approaches and fluid rich polymer networks, we propose fabrication of composite materials following the approach of incorporating liquid fillers self-enclosed within a polymer matrix (**Figure 1**b). An appropriate choice of liquid filler with interfacial compatibility dispersed as globular phases within the elastomer matrix, mimicking a skin-like structure, could improve the dielectric constant, provide thermal and ambient stability and mitigate issues like mechanical stiffening and reduced stretchability.

Herein, we report a self-enclosed liquid filler (SELF) composites with ionic liquid (1-Ethyl-3-methylimidazolium bis (trifluoromethylsulfonyl) imide (EMIMTFSI)) as a novel liquid filler inside polydimethylsiloxane (PDMS) polymer matrix, resulting in synergetic effects on the dielectric and mechanical properties of the resulting composite. An unprecedented 100 times decrease in the Young's modulus and a remarkable 360% increase in the ultimate strain indicates the substantial role of the liquid fillers in the composite. The liquid fillers almost double the dielectric constant of the composite. The high thermal stability and non-volatile nature of the ionic liquid fillers lend the composites excellent stability over hydrogels, even at elevated temperatures and also endow the composite with high transparency (82–90%). Employed as a capacitive pressure sensor, these composites show an impressive sensitivity of 32.86 Pa^{-1} without the aid of any microstructuring. Owing to the synergistic improvement in dielectric constant and mechanical properties, DEAs fabricated from the composite displays 2.5 times improvement in longitudinal strains produced and 4 times improvement in areal strains at half the electric fields compared to state-of-the-art acrylic films. These composites could enable combined sensing and actuation utilizing a single material system and novel shape morphing systems producing large strains at low electric fields.

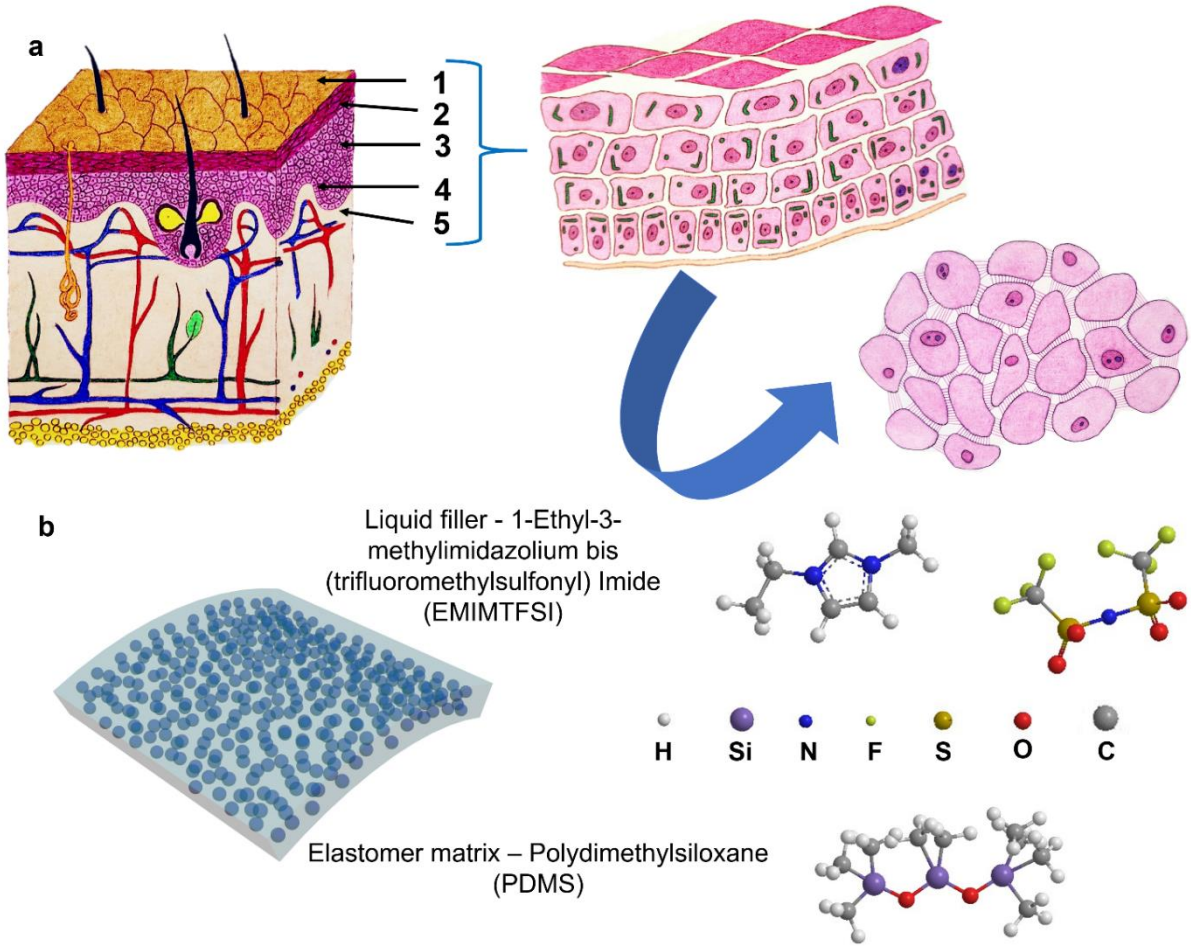

Figure 1. (a) (Left) Schematic of human skin. Different layers in epidermis are labelled. (1- Stratum Corneum, 2- Stratum Lucidium,3- Stratum Granulosum, 4- Stratum Spinosum, 5- Stratum Basale). These layers have different compositional structures with varying concentration of fluids amongst them, leading not only to different functionalities but different mechanical properties as well. (Right) An enlarged schematic of epidermis showing the different layers with a detailed schematic of the stratum granulosum, made of cells and lipids filling the intracellular spaces. (b) Schematic of the proposed SELF composite, where the liquid fillers exist as separated globular phases inside the polymer matrix. The chemical structure of the proposed liquid filler (EMIMTFSI) and polymer matrix (PDMS) is represented on the right.

RESULTS AND DISCUSSION

Principles of design and Choice of liquid fillers:

Electric field driven soft actuators require a stable soft elastomeric material with enhanced dielectric constant and reduced mechanical stiffness. PDMS (**Figure 1**b) was chosen as the host elastomer due to its cost effectiveness, biocompatibility, good viscoelastic properties and facile fabrication suitable for large scale manufacturing[16]. Effective medium theory

approximations indicate that a composite's dielectric constant lies between that of its individual constituents (**Figure 2**a)[19, 26-27]. Ionic liquids (ILs) are essentially salts which are liquid at ambient temperatures[28]. Aprotic ionic liquids like EMIMTFSI (**Figure 1**b) possess high dielectric constants (in the range of 10-12), a large electrochemical window and very high decomposition temperatures which make them attractive for electrochemical applications[28-29].

The mechanical stiffness of solid composites with liquid fillers could be predicted by extending Eshelby's theory (dilute filler concentrations)[30] and Mori-Tanaka approximations (non-dilute filler concentrations). However, they both neglect the effect of surface tension and interfacial stresses[31], crucial for solid-liquid matrices. Style's model[32] which accounts for such interfacial effects was therefore utilised to estimate the mechanical stiffness of EMIMTFSI-PDMS composites (**Figure 2**b). The mechanical stiffness is linked to the elastocapillary length (ratio of surface tension to the Young's modulus) which can be modulated by the choice of liquid filler and the bulk matrix[32]. In the case considered here, for small radii of inclusion (~100-250nm), the surface tension effects are significant, resisting the deformation of liquid inclusions to keep them spherical. At radii exceeding 1 micron, the surface tension is overwhelmed by bulk elasticity – enabling access to a regime of reduced Young's modulus values, lower than even the host polymer matrix.

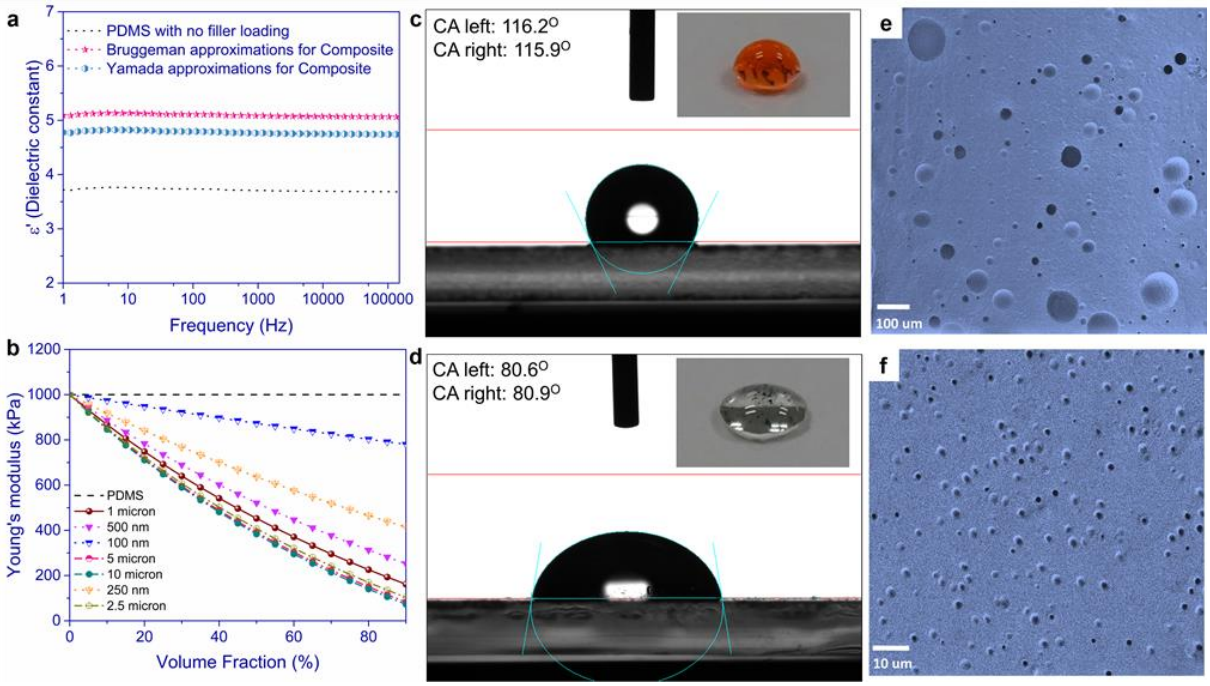

Figure 2. (a) Approximated dielectric constant values of the EMIMTFSI-PDMS composites using Bruggeman's model and Yamada's model at different frequencies. Dielectric constant of PDMS matrix at different frequencies as measured by dielectric spectroscopy. (b) Prediction of elastic modulus of the composite by Style et. al.'s extension of the Eshelby's theory within Mori-Tanaka multiphase approximation. (c) Bitmap image of contact angle measurement for water on PDMS membrane (116^o). (Inset) Image of a water droplet (with red dye) and an EMIMTFSI droplet on PDMS. The water droplet maintains a strong spherical shape, indicative of a large contact angle, low interfacial tension and incompatibility of the materials. (d) Bitmap image of contact angle measurement for EMIMTFSI on PDMS membrane (80^o). The EMIMTFSI droplet spreads out on the surface, indicating small contact angle which signifies high interfacial tension and compatibility of the materials. Cross-sectional scanning electron micrographs of (e) PDMS+Water mixture (10%) showing the uneven filler distribution (Scale bar – 100 microns) and (f) PDMS+EMIMTFSI (10%) showing uniform filler distribution in the composite (Scale bar – 10 microns). Liquid filler phases can be observed clearly as spherical inclusions inside the polymer matrix.

The dielectric and mechanical predictions clearly show the potential of SELF composites. However, the mixing of a liquid and a solid phase poses challenge of phase segregation and processability. If the liquid filler has poor compatibility with the solid matrix, the composite will suffer from phase separation, segregation and non-uniform filler size distribution (**Figure S2**a). This in turn leads to undesirable high viscosities, poor dispersion and poor mechanical properties. For the liquid to form self-contained inclusions within the polymer matrix, the nature of interaction between the liquid and the matrix is crucial. Compatibility between phases

can be estimated from contact angle measurements. The contact angle of water on PDMS is high (116^{o}, **Figure 2**c), with high contact angles indicating low interfacial tension. This results in phase segregation and filler size variation in the composite, leading to no observable trends in stress-strain behavior with increasing filler concentration (**Figure S3**). The interaction between EMIMTFSI and PDMS was more favorable with a lower contact angle (~80^{o}, **Figure 2**d). This in-turn leads to uniform filler size distribution in the composite (**Figure S2** b). We capitalize on the immiscibility of the two systems and favorable interaction between the phases to create self-contained globules of EMIMTFSI inside the PDMS matrix. These globular filling structures are very stable and sustain large strains applied by either stretching or compressing; and no leakage was observed (**Figure S4** and **S5**). Scanning electron microscopy (SEM) images show the morphology for Water-PDMS (**Figure 2**e) and EMIMTFSI-PDMS (**Figure 2**f) composites at 10% filler loading fabricated by shear mixing. In congruence with the contact angle dependencies, the fillers are distributed uniformly within the EMIMTFSI-PDMS composite and are much smaller (~1um) in size as compared to the Water-PDMS composite. Optical microscopy images (**Figure S6**) confirm the uniform distribution of the globular phases while Fourier-transform infrared spectroscopy (FTIR) measurements indicate that the ionic liquids maintain their chemical composition (**Figure S7**).

Synergetic effect on Dielectric constant and Young's modulus:

Dielectric spectroscopy for the EMIMTFSI-PDMS matrices (**Figure 3**a and **Figure S8**) shows an impressive increase of around 200% in the dielectric constant value for PDMS+EMIMTFSI (20%) over the pristine PDMS matrix. For all frequencies, there is an increase in the ε' with increasing concentration of EMIMTFSI. The PDMS+EMIMTFSI (20%) has a dielectric constant of ~7 compared to the value of 3.7 for pristine PDMS matrix. The dielectric constant increases with ionic liquid concentration, with values of 5, 5.5 and 6.45 obtained for 5%, 10% and 15% loading. The high dielectric constant is attributed to the space charge polarization of

ionic species self-contained in the heterogeneous composite material[26, 28]. Examining the imaginary part of relative permittivity (ε") reveals no increase in the loss factor with increasing ionic liquid concentration. This could originate from the discreteness of the EMIMTFSI globular phases within the PDMS matrix that hinders an ionic conduction path. Complex conductivity for different concentrations of ionic liquid shows minor change over the frequency range. With change in the electrode area, the dielectric behavior remains the same with no significant variations (**Figure S9**). We expect that scaling down to even lower sizes, comparable to size of globular EMIMTFSI inclusions, may lead to some variation in the observed dielectric behavior.

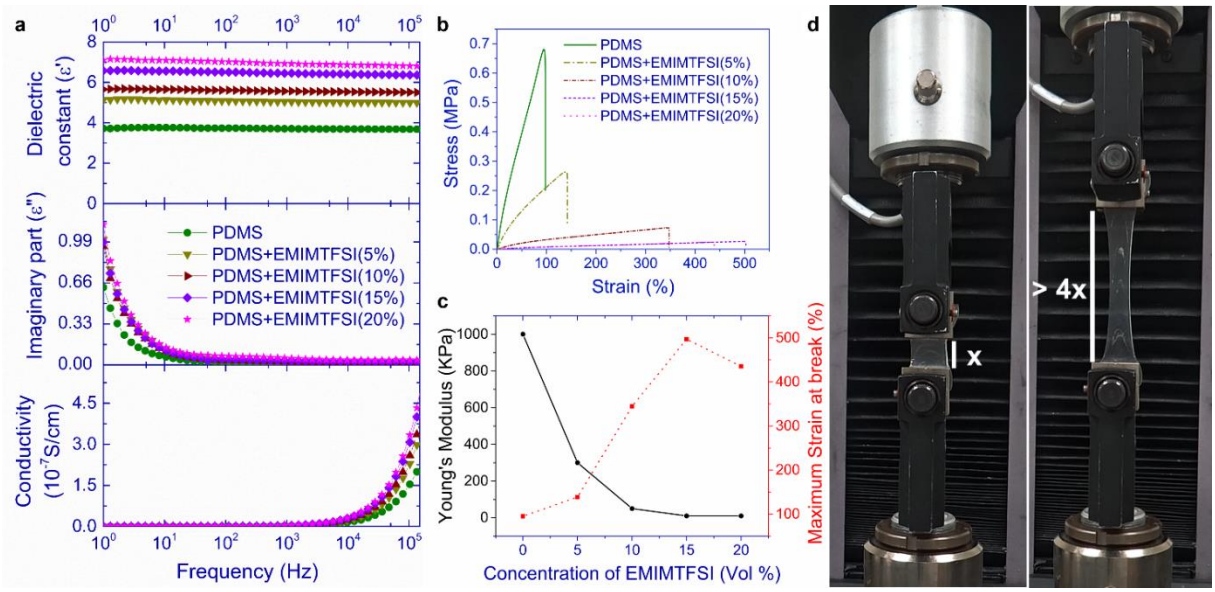

Figure 3. Synergetic effect on Dielectric constant and Young's modulus. (a) Plot of dielectric constant (real part of permittivity), imaginary part and conductivity against frequency with increase in EMIMTFSI concentration. (b) Stress-strain curves obtained by Uniaxial tensile tests for composites with different EMIMTFSI concentrations. Softening of the matrix can be clearly observed from the curves. (c) Plot of Young's modulus (300 kPa, 50 kPa and 10 kPa at 5%, 10% and 15% filler loading respectively) and maximum strain at break against filler concentration. Decrease in Young's modulus can be observed with increasing EMIMTFSI concentration; whereas the maximum strain at break increases with increasing EMITFSI concentration, till it reaches a minimum value at 15% filler loading. (d) Image of PDMS+EMIMTFSI (20%) stretched more than 400% of its initial length using Uniaxial tensile testing apparatus.

Figure 3b shows the stress-strain curve measured for EMIMTFSI-PDMS composites for varying filler concentrations. The slope of the stress-strain curves (**Figure 3**b) reduces with

increasing concentration of EMIMTFSI. The Young's modulus decreases to 10 kPa for PDMS+EMIMTFSI (20%) compared to 1 MPa for pristine PDMS (**Figure 3**c) resembling soft, biological materials[1]. Previous reports have shown reduction in stretchability of the composites with solid filler addition, whereas our unique liquid filler system shows an impressive improvement in the maximum strain at break for all concentrations (**Figure 3**d and **Movie S1**). PDMS showed an ultimate strain of 95%, while the addition of 20% EMIMTFSI increased the ultimate strain by 4.6 times to 435%. The maximum ultimate strain value of 497% is achieved at a concentration of 15%; with stretchability of the composite starting to decline subsequently. The unique set of dielectric and mechanical properties achieved by EMIMTFSI-PDMS composites compared to other reports (**Table 1**) can be attributed to the unique self-enclosed nature of the liquid fillers. Composites for DEAs have been benchmarked by a figure of merit (F.O.M.) for electro-mechanical performance (**Table S1**)[19]. The PDMS+EMIMTFSI (20%) composites show an impressive F.O.M. of 187, two orders of magnitude higher than composites fabricated with ceramic fillers. Dielectric properties of the composite remained similar for varying film thickness, but a slight variation in the mechanical properties was observed with variation in film thickness (**Figure S10**). Although there are no general expressions relating dielectric constant and Young's modulus of a material with its electrical breakdown strength; an empirical relation based on Maxwell-stress actuation suggests a reduction in electrical breakdown strength with increase in dielectric constant and reduction in Young's modulus[33]. Hence, for the EMIMTFSI-PDMS composites, the increase in dielectric constant and reduction in Young's modulus is accompanied with reduction in electrical breakdown strength. Electrical breakdown measurements (**Figure S11**) were done for 13 different samples of the PDMS+EMIMTFSI (20%) composite and an average breakdown strength of ~15 V/μm was recorded.

Table 1. Comparison of electrical and mechanical properties of EMIMTFSI-PDMS composites against other elastomeric composites. Synergetic increase in dielectric constant and reduction in Young's modulus is achieved with increase in the stretchability by the SELF composites.

Elastomer matrix	***Filler***	***Filler attribute***	***Filler loading***	***Dielectric constant @ 1 kHz***	***Young's modulus (MPa)***	***Ultimate strain at break (%)***	***Reference***
PDMS [Sylgard 184]	EMIMTFSI	Liquid; Ionic	Pristine	**3.7**	**1**	**95**	Current work
			20% by volume	**~7**	**0.01**	**435**	
SEBS [Poly (styrene-ethylene-butadiene-styrene)]	PU [Polyurethane]	Solid; Polymeric; Dielectric	Pristine	**2.7**	**0.8**	**811**	Bolados et al, 2019[34]
			10% by weight	**4.0**	**2.1**	**802**	
Acrylonitrile butadiene rubber [NBR]	Poly(dopamine) and silane surface functionalized TiO_2 nanoparticles	Solid; Ceramic	Pristine	**~13.5**	**~1.375**	**~250**	Yang et al, 2016[35]
			30 phr [parts per hundred parts of rubber]	**~15.75**	**~1.475**	**~350**	
PDMS [Sylgard 184]	Glycerol	Liquid	Pristine	**3.3**	**1.07**	**154**	Mazurek et al, 2016[36-37]
			50% by volume	**~16**	**0.33**	**116**	
PDMS [Sylgard 184]	Eutectic Gallium Indium nanoparticles	Liquid; Conductive; Metallic	Pristine	**~3**	**~1.5**	**~150**	Pan et al, 2019[38]
			20% by volume	**~8**	**~2**	**160**	

Stability, Transparency and Pressure sensing:

Ionic liquids have high decomposition temperatures and insignificant vapor pressures[29]. This lends superior stability to the PDMS+EMIMFTSI composites in both extreme and ambient conditions, compared to hydrogels. **Figure 4**a shows the TGA (Thermogravimetric Analysis) plot for the composites (50^{o}C to 600^{o}C) against hydrogels (30^{o}C to 450^{o}C) to evaluate the decomposition onset. Hydrogels show rapid weight loss at low temperatures, completely losing water by 100^{o}C due to the facile rupture of weak hydrogen bonds [39-40]. The onset temperature for the EMIMTFSI-PDMS composites lies above 300^{o}C with negligible change in the onset temperature for increasing EMIMTFSI concentration (**Figure S12**) testifying its thermal stability. EMIMTFSI-PDMS composites show impressive ambient stability (RH – 60%), with no weight change measured over 12 days, indicating no environmental moisture uptake and no volatile weight loss of the filler (**Figure 4**b). The hydrogels lost all water content within 3 days in ambient leading to significant variation in the measured mechanical properties (**Figure S13**). Hence, the self-contained liquid filler morphology of the SELF composites results in high stability compared to hydrogels. Transparency @ 550 nm is measured at ~95% for PDMS+EMIMTFSI (5%) and decreases gradually to ~ 82% for PDMS+EMIMTFSI (20%) (**Figure 4**c, d). Refractive index contrast as well as filler size and shape are critical in determining light scattering and hence transparency limiting performance in solid filler-based composites.[41] The closely matched refractive indices for PDMS (1.4118) and EMIMTFSI (1.4272) and the smaller filler size results in minor light scattering effects. Transparency of the composite was found to be dependent on the film thickness and transmittance decreased with an increase in the film thickness (**Figure S14**).

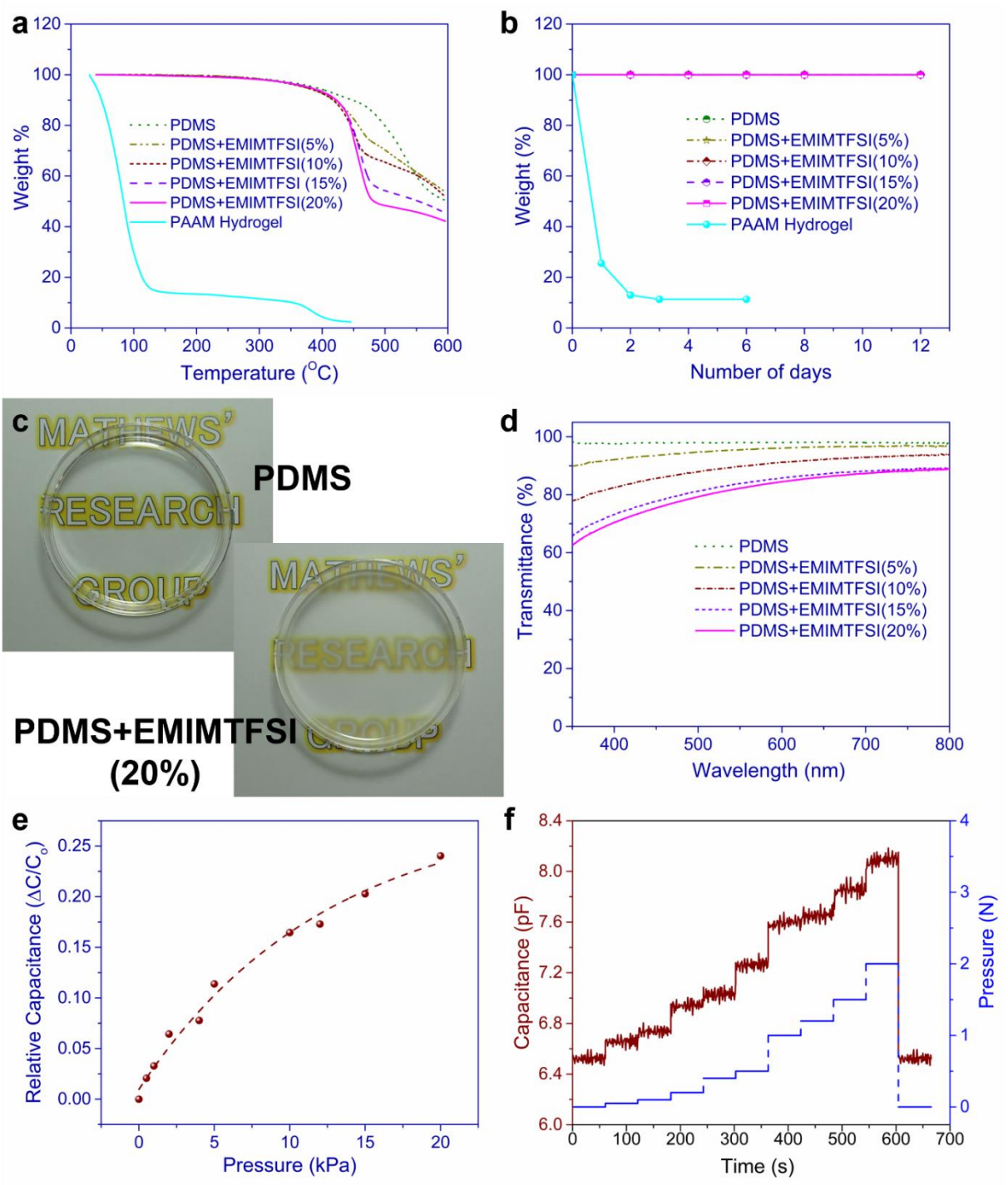

Figure 4. Stability, Transparency and Pressure sensing. (a) TGA plots for pristine PDMS, EMIMTFSI-PDMS composites (50°-600°C) and PAAM hydrogel (30°-450°C). PAAM hydrogels lose all the fluid content as temperature reaches 100°C, while the onset temperature for EMIMTFSI composites lies above 300°C. (b) Plot of weight percentage versus number of days to observe the effect of moisture uptake or volatile losses. No change in weight is found for EMIMTFSI-PDMS composites for 12 days. Hydrogel loses all its water content from the network in 3 days. (c) Pristine PDMS and PDMS+EMIMTFSI (20%) samples in a petri dish kept in front of an image highlighting the transparency of the films. (d) Transmittance versus wavelength plot from the UV-Vis measurements. Plot shows the transparency of the pristine PDMS and EMIMTFSI-PDMS composites with different filler concentrations in the visible spectrum. (e) Plot of relative variation in capacitance with change in applied pressure for

calculating the sensitivity. High sensitivity of 0.03286 kPa^{-1} is obtained in low-pressure regime. (Inset) Image of a capacitive pressure sensor (active area – 1cm x 1cm) with etched FTO glass as the bottom substrate and electrode, 2.25 mm thick PDMS+EMIMTFSI (20%) film as the dielectric layer and spray-coated AgNW as the top electrode. (f) Plot of change in absolute capacitance with time and applied pressure.

Owing to the attractive optical, dielectric and mechanical properties, a transparent capacitive pressure sensor[42-43] was constructed with a 2.25 mm thick PDMS+EMIMTFSI (20%) layer sandwiched between transparent conducting electrodes (**Figure 4**e, inset). Relative variation in capacitance is plotted in **Figure 4**e with respect to applied pressure and allows for extraction of pressure sensitivity [44]. In the low-pressure regime from 0 – 1 kPa, the sensitivity is calculated to be 0.03286 kPa^{-1}, for the 1 kPa – 5 kPa regime, the sensitivity changes to 0.02024 kPa^{-1}; while for the high-pressure regime (10 kPa – 20 kPa), the sensitivity is calculated to be 0.00757 kPa^{-1}. Typically, the sensitivity of capacitive pressure sensors is increased by micro-structuring, which increases fabrication complexity and opaqueness.[44] The sensitivity obtained with these thick PDMS+EMIMTFSI (20%) films compare favourably to recent reports, even without microstructuration[44-46]. **Figure 4**f shows the variation of measured capacitance with time and applied pressure. Capacitance remains stable over time and follows the pressure curve, and immediately returns to original state after pressure removal (**Figure 4**f and **Movie S2**) with no hysteresis. The sensor showed no observable hysteresis in the measured capacitance when subjected to sequential loading and unloading of weights (**Figure S15**).

Actuation performance:

Finally, the performance of these composites in an actuator configuration was evaluated. Skeletal muscles contracts either by shortening (concentrically) or lengthening (eccentrically) in isometric and isotonic configurations, and differ in terms of force generation mechanism, maximum force production and energy cost[47]. Isotonic configurations are known to generate greater force than isometric and concentric contractions, at a lower metabolic cost[47]. Hence, the actuation performance of the PDMS+EMIMTFSI (20%) composite was characterized in a

non-prestretched pure shear isotonic configuration[33] (**Figure 5**a) with a fixed load of 50 grams (0.4903 N~500 mN) and compared to the conventionally used DEA material (Acrylic tape, 3M VHB 4910). An actuation stroke of more than 5 mm (0.5 cm) was achieved by the composite, exceeding VHB (**Figure 5**b, c). **Figure S16** shows the longitudinal actuation strains for applied voltages, with PDMS+EMIMTFSI (20%) composite (3.32%) showing ~2.5 times better performance than VHB 4910 (1.35%) at 8kV. This reaffirms our strategy of pursuing materials development for simultaneous improvements in dielectric constant and reduced mechanical stiffness. The performance improvement is even more clear when the thickness of the two films (1 mm for VHB, 2.5mm for PDMS+EMIMTFSI (20%)) are accounted for, by considering the nominal electric field (**Figure 5**d). We observe an increase of ~2.5 times in the strain produced at nearly half the nominal applied electric field (3.6 V/μm for PDMS+EMIMTFSI (20%) compared to 8 V/μm for VHB), making a 5 times improvement in the actuation performance. Similarly, an 8 times effective improvement in the areal strain (**Figure 5**d and **Figure S16**) is noted. Reduction in actuation strain with increasing load was also observed, which is a characteristic of mammalian muscle [2]. At a fixed load of ~300 mN, the PDMS+EMIMTFSI (20%) composite showed 2 times more longitudinal strain compared to the strain produced with a fixed load of 500 mN (**Figure 5**e) (2.9% at 500 mN load against 5.35% at 300 mN load, applied voltage – 6kV, film thickness – 2.25 mm). The actuation of PDMS+EMIMTFSI (20%) in isotonic configuration is shown in **Movie S3**.

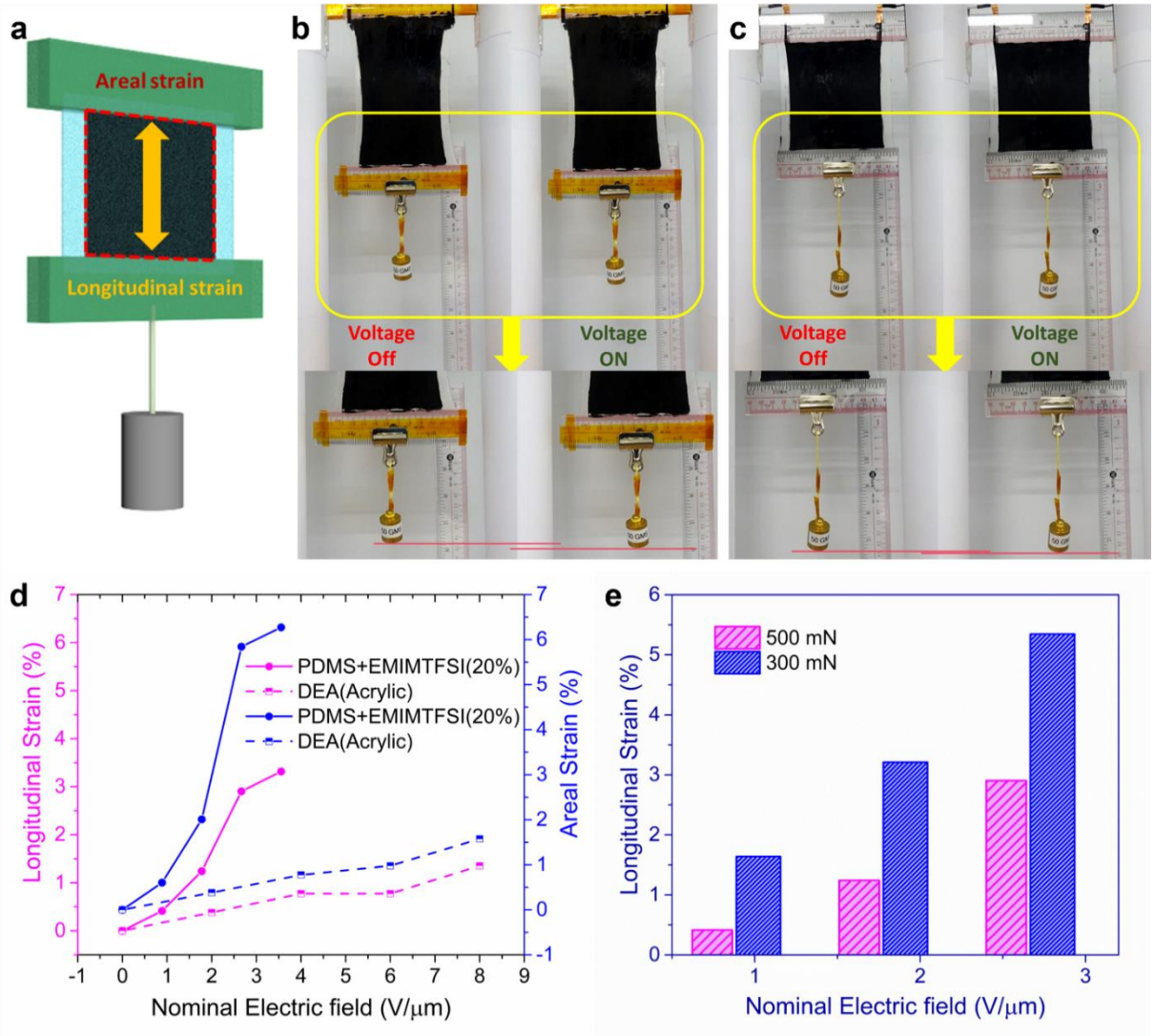

Figure 5. Actuation Performance. (a) Schematic of Pure-shear, Isotonic configuration of DEAs. Digital image of (b) PDMS+EMIMTFSI (20%) and (c) VHB 4910 devices with 50 grams (~0.5 N) load hanging from them. Digital image of the actuated devices under applied voltage (8 kV) are shown next to them. (d) Longitudinal and areal strain produced versus applied nominal electric field. PDMS+EMIMTFSI (20%) composites show 2.5 times improvement in longitudinal strain and 4 times improvement in areal strain compared to conventional acrylic films (VHB 4910) at only 1/2 the nominal electric field, making effective improvement in actuation performance 5 times and 8 times, respectively. (e) Variation in longitudinal strain with applied nominal electric field at different loading conditions.

Thus, the EMIMTFSI-PDMS composites show an enhanced performance against conventionally used acrylates (3M VHB) in terms of actuation strains (**Movie S4**); standing in good stead against other chemical and filler modifications of polymer backbones.[16, 19, 48] The actuation performance compares well against other recent reports of field-driven actuators, at significantly low electric field (**Table 2**). Actuator shows high durability by maintaining its

performance over 500 cycles (**Figure S17**). The significant improvements in the actuation performance in non-prestretched configurations demonstrated here, opens the possibility of employing these composites for low-field driven shape morphing devices.

Table 2. Comparison of actuation performance of EMIMTFSI-PDMS composites against state-of-the-art dielectric elastomer actuators. The actuation performance bodes well against others at significantly lower electric field.

Material system for active layer	***Pre-stretching***	***Actuation strain (%)***	***Applied Electric field (V/µm)***	***Reference***
EMIMTFSI-PDMS self-enclosed composites	No	**3.3** (longitudinal strain) **6.27** (Areal strain)	~**3.5**	Current work
Biaxially oriented polypropylene (BOPP) pouches filled with dielectric field	No	**~10** (longitudinal strain)	**240**	Kellaris et al, 2018[49]
UV curable acrylates	No	**~5** (Areal strain)	**20**	Duduta et al, 2016[50]; Duduta et al 2019[3]
Acrylic based dielectric gel	Yes (1.5*1.5)	**~12** (longitudinal strain)	**~9** (estimated)	Shi et al 2018[51]
VHB 4910	No	**1.35** (longitudinal strain) **1.58** (Areal strain)	**8**	Current work

CONCLUSION

Drawing inspiration from soft biological materials, we successfully demonstrated the fabrication of self-contained ionic liquid filler-polymer composite with EMIMFTSI as the liquid filler and PDMS as the polymer matrix. These liquid fillers exist in globular phases, separated from each other, inside the polymer matrix. Addition of EMIMTFSI fillers leads to

synergetic effect on the electrical and mechanical properties, showing an increase of ~1.9 times in the dielectric constant with no change in the loss behaviour and a decrease of 100 times in the Young's modulus. This is accompanied by 4.6 times increase in the maximum strain at break (stretchability). A figure of merit of 187 is calculated for the electromechanical performance of the fabricated composite. Additionally, these composites show excellent thermal and moisture stability along with high transparency. These soft, high dielectric constant composites allow the fabrication of highly sensitive pressure sensors without the need for microstructuring. Finally, these composites actuated in a non-prestretch pure shear isotonic DEA configuration showed superior performance compared to conventionally used acrylics. An effective improvement in longitudinal strain (5 times) and areal strain (8 times) is also demonstrated, with nominal electric fields as low as 4V/μm. In addition to applications in soft robotics, this class of self-enclosed ionic liquid polymer composites would impact the areas of shape morphing, electronic skins and optoelectronic devices[52-53].

MATERIALS AND METHODS

Materials fabrication and characterization:

1-Ethyl-3-methylimidazolium bis (trifluoromethylsulfonyl) imide (EMIMTFSI) (Sigma Aldrich) was utilized, as received, to fabricate the self-contained liquid-filler polymer composite with polydimethylsiloxane (PDMS) (Sylgard 184, Dow Corning) as the polymer matrix. The EMIMTFSI-PDMS composites were fabricated by shear mixing in a planetary mixer (Thinky, ARE310), drop casted in a petri-dish and cured in an oven (50^{o}C, Memmert). No additional fabrication step was needed to ensure enclosure of EMIMTFSI phases within the PDMS matrix. There was no migration of EMIMTFSI droplets towards the top or bottom surface during the curing process (**Figure S18**). Water-PDMS composites were fabricated by shear mixing DI water into the PDMS matrix. Nature of interaction between the EMIMTFSI

fillers and the PDMS matrix were determined by contact angle measurements (DataPhysics, OCA 15Pro) and FTIR (Thermo Scientific, Nicolet Continuum). Size of the fillers and distribution of filler size were analysed by scanning electron microscopy (JSM-7600F) and optical microscopy (Olympus, CX31-P). Real and imaginary parts of the relative permittivity were extracted from the dielectric spectroscopy performed on a dielectric spectrometer (Novocontrol, Alpha "A" Analyzer). Uniaxial tensile tests were performed to extract the mechanical properties (C42, MTS Criterion Systems).

Effect of filler size and distribution:

Our emphasis on filler size and distribution, which motivated the choice of liquid filler, is also borne out in the choice of the fabrication process. The fabrication technique affects the filler size distribution in the matrix, in turn affecting the electromechanical properties. The increase in ε' with filler loading is observed for both uniform and non-uniform filler size distribution. However, uniform filler size distribution, achieved by the shear mixing process (planetary mixing), results in higher dielectric constant at lower EMIMTFSI concentration (**Figure S19**a, Supplementary Information) as compared to manual mixing. The positive effect of uniform filler size distribution is also observed on the mechanical properties of the matrix. With even filler size distribution, a Young's modulus of 10 kPa is achieved at 15% filler loading itself (**Figure S19**b, Supplementary Information); compared to the Young's modulus of 20 kPa obtained for 25% filler loading for uneven filler size distribution (**Figure S19**c, Supplementary Information). It should be noted that even filler size distribution also contributes to better F.O.M. compared to the uneven filler size distribution (84.7).

Device fabrication and characterization:

Capacitive pressure sensor device was fabricated on etched FTO glass (substrate and bottom electrode) with spray coated silver nanowires as top electrodes with a 2.25 mm thick

PDMS+EMIMTFSI (20%) film. Changes in the relative capacitance were monitored using an LCR meter (Keysight, E4980A Precision) and captured in the demonstration using an evaluation board (Analog Devices, EVAL-AD7150). Higher sensitivities can be obtained by miniaturization of overlapping electrode area and reduction of film thickness. Actuators were fabricated using 2.25 mm thick PDMS+EMIMTFSI (20%) film and 1 mm thick VHB 4910 acrylic film (lateral dimensions 12 cm x 12 cm) with carbon paste electrodes (electrode area – 10 cm x 10 cm). Electric field was applied to the devices by controlling the step-up transformer (XP Power, CB101), which received the input voltage and monitor voltage by a DC voltage supply (Aim-TTi, MX100TP). Strain measurements were done by capturing images (SONY, α6300 E-mount) and analyzing them using Image J (FIJI) image processing software.

ASSOCIATED CONTENT

Supporting Information

The following files are available free of charge.

Supporting Information (pdf) – Supporting information contains Basic configuration of Dielectric elastomer actuators (DEAs); Effective medium theories for dielectric approximation; Eshelby's theory and its extensions for liquid inclusions in solid matrix; Schematic of composites; Effect of type of filler on mechanical properties; Globular filling structures resisting tension; Globular filling structures resisting compression; Optical microscopy images; FTIR spectroscopy; Electric circuit equivalent of DEA; Effect of electrode area on relative permittivity (dielectric constant); Figure of merit; Effect of film thickness on mechanical and dielectric properties; Electrical breakdown in PDMS+EMIMTFSI (20%) composite; Thermogravimetric analysis – onset temperature; Effect of water content on mechanical properties of PAAM hydrogels; Effect of thickness of PDMS+EMIMTFSI (20%) film on transmittance; Hysteresis free performance of pressure sensor while sequential loading and unloading; Actuation performance: actuation strain versus applied voltage; Cyclic actuation performance; SEM Image of top and bottom surface and Effect of filler size distribution on electromechanical properties.

Movie S1 - Stretchability of PDMS+EMIMTFSI (20%) film.

Movie S2 - Pressure sensing using PDMS+EMIMTFSI (20%) film.

Movie S3 - Actuation of PDMS+EMIMTFSI (20%) film.

Movie S4 - Comparison of actuation performance.

Author contributions

Ankit conceived the initial idea with the guidance from N.M. Ankit designed and led the research, carried out the experiments, and analysed the experimental and theoretical model data, under the supervision of N.M. N.T. helped with the FTIR spectroscopy. F.H. prepared the samples for uneven size distribution of liquid fillers. F.K. prepared the schematic sketches for the manuscript and helped in arrangement of figures. M.R.K. helped in pressure sensor characterization. L.L.N. prepared the hydrogel samples. K.S.J.A. helped in carrying out the dielectric spectroscopy measurements. Ankit wrote the manuscript. All the authors contributed in reviewing the manuscript.

Notes

The authors declare no competing financial interest.

AUTHOR INFORMATION

Corresponding Author

Nripan Mathews

*Email – nripan@ntu.edu.sg.

ACKNOWLEDGEMENTS

The authors would like to acknowledge funding from the Ministry of Education (MOE) Tier 1 grant (MOE2018-T1-002-179).

References

1. Rus, D.; Tolley, M. T., Design, Fabrication and Control of Soft Robots. *Nature* **2015,** *521*, 467-475.
2. Acome, E.; Mitchell, S. K.; Morrissey, T. G.; Emmett, M. B.; Benjamin, C.; King, M.; Radakovitz, M.; Keplinger, C., Hydraulically Amplified Self-Healing Electrostatic Actuators with Muscle-like Performance. *Science* **2018,** *359* (6371), 61-65.

3. Duduta, M.; Hajiesmaili, E.; Zhao, H.; Wood, R. J.; Clarke, D. R., Realizing the Potential of Dielectric Elastomer Artificial Muscles. *Proceedings of the National Academy of Sciences* **2019,** *116* (7), 2476-2481.
4. Haines, C. S.; Lima, M. D.; Li, N.; Spinks, G. M.; Foroughi, J.; Madden, J. D. W.; Kim, S. H.; Fang, S.; Jung de Andrade, M.; Göktepe, F.; Göktepe, Ö.; Mirvakili, S. M.; Naficy, S.; Lepró, X.; Oh, J.; Kozlov, M. E.; Kim, S. J.; Xu, X.; Swedlove, B. J.; Wallace, G. G.; Baughman, R. H., Artificial Muscles from Fishing Line and Sewing Thread. *Science* **2014,** *343* (6173), 868-872.
5. Miriyev, A.; Stack, K.; Lipson, H., Soft Material for Soft Actuators. *Nature Communications* **2017,** *8* (1), 596.
6. Shintake, J.; Cacucciolo, V.; Floreano, D.; Shea, H., Soft Robotic Grippers. *Advanced Materials* **2018,** *30* (29), 1707035.
7. Hu, W.; Lum, G. Z.; Mastrangeli, M.; Sitti, M., Small-Scale Soft-Bodied Robot with Multimodal Locomotion. *Nature* **2018,** *554*, 81–85.
8. Shepherd, R. F.; Ilievski, F.; Choi, W.; Morin, S. A.; Stokes, A. A.; Mazzeo, A. D.; Chen, X.; Wang, M.; Whitesides, G. M., Multigait Soft Robot. *Proceedings of the National Academy of Sciences* **2011,** *108* (51), 20400-20403.
9. Xu, C.; Stiubianu, G. T.; Gorodetsky, A. A., Adaptive Infrared-Reflecting Systems Inspired by Cephalopods. *Science* **2018,** *359* (6383), 1495-1500.
10. Ankit; Tiwari, N.; Rajput, M.; Chien, N. A.; Mathews, N., Highly Transparent and Integrable Surface Texture Change Device for Localized Tactile Feedback. *Small* **2018,** *14* (1), 1702312.
11. Pelrine, R.; Kornbluh, R.; Pei, Q.; Joseph, J., High-Speed Electrically Actuated Elastomers with Strain Greater Than 100%. *Science* **2000,** *287* (5454), 836-839.
12. Keplinger, C.; Sun, J.-Y.; Foo, C. C.; Rothemund, P.; Whitesides, G. M.; Suo, Z., Stretchable, Transparent, Ionic Conductors. *Science* **2013,** *341* (6149), 984-987.
13. Ankit, A.; Chan, J. Y.; Nguyen, L. L.; Krisnadi, F.; Mathews, N., *Large-Area, Flexible, Integrable and Transparent DEAs for Haptics*. SPIE: 2019; Vol. 10966.
14. She, A.; Zhang, S.; Shian, S.; Clarke, D. R.; Capasso, F., Adaptive Metalenses with Simultaneous Electrical Control of Focal Length, Astigmatism, and Shift. *Science Advances* **2018,** *4* (2), eaap9957.
15. Jun, S.; Vito, C.; Herbert, S.; Dario, F., Soft Biomimetic Fish Robot made of Dielectric Elastomer Actuators. *Soft Robotics* **2018,** *5* (4), 466-474.
16. Romasanta, L. J.; Lopez-Manchado, M. A.; Verdejo, R., Increasing the Performance of Dielectric Elastomer Actuators: A Review from the Materials Perspective. *Progress in Polymer Science* **2015,** *51*, 188-211.
17. Brochu, P.; Pei, Q., Advances in Dielectric Elastomers for Actuators and Artificial Muscles. *Macromolecular Rapid Communications* **2010,** *31* (1), 10-36.
18. Qiu, Y.; Zhang, E.; Plamthottam, R.; Pei, Q., Dielectric Elastomer Artificial Muscle: Materials Innovations and Device Explorations. *Accounts of Chemical Research* **2019,** *52* (2), 316-325.
19. Romasanta, L. J.; Leret, P.; Casaban, L.; Hernández, M.; de la Rubia, M. A.; Fernández, J. F.; Kenny, J. M.; Lopez-Manchado, M. A.; Verdejo, R., Towards Materials with Enhanced Electro-Mechanical Response: CaCu3Ti4O12–Polydimethylsiloxane Composites. *Journal of Materials Chemistry* **2012,** *22* (47), 24705-24712.
20. GUZMÁN-ALONSO, M.; CORTAZÁR, T. M., Water Content at Different Skin Depths. *Household and Personal Care Today* **2016,** *11*.
21. Hanson, D.; Bergs, R.; Tadesse, Y.; White, V.; Priya, S., *Enhancement of EAP Actuated Facial Expressions by Designed Chamber Geometry in Elastomers*. SPIE: 2006; Vol. 6168.

22. Mackenzie, I. C., Ordered Structure of The Epidermis. *Journal of Investigative Dermatology* **1975,** *65* (1), 45-51.
23. Sun, J.-Y.; Zhao, X.; Illeperuma, W. R. K.; Chaudhuri, O.; Oh, K. H.; Mooney, D. J.; Vlassak, J. J.; Suo, Z., Highly Stretchable and Tough Hydrogels. *Nature* **2012,** *489* (7414), 133-136.
24. Matsumoto, K.; Sakikawa, N.; Miyata, T., Thermo-Responsive Gels that Absorb Moisture and Ooze Water. *Nature Communications* **2018,** *9* (1), 2315.
25. Markvicka, E. J.; Bartlett, M. D.; Huang, X.; Majidi, C., An Autonomously Electrically Self-Healing Liquid Metal–Elastomer Composite for Robust Soft-Matter Robotics and Electronics. *Nature Materials* **2018,** *17* (7), 618-624.
26. Markel, V. A., Introduction to the Maxwell Garnett Approximation: Tutorial. *J. Opt. Soc. Am. A* **2016,** *33* (7), 1244-1256.
27. Yamada, T.; Ueda, T.; Kitayama, T., Piezoelectricity of a High-Content Lead Zirconate Titanate/Polymer Composite. *Journal of Applied Physics* **1982,** *53* (6), 4328-4332.
28. Huang, M.-M.; Jiang, Y.; Sasisanker, P.; Driver, G. W.; Weingärtner, H., Static Relative Dielectric Permittivities of Ionic Liquids at 25 °C. *Journal of Chemical & Engineering Data* **2011,** *56* (4), 1494-1499.
29. Fröba, A. P.; Kremer, H.; Leipertz, A., Density, Refractive Index, Interfacial Tension, and Viscosity of Ionic Liquids [EMIM][EtSO4], [EMIM][NTf2], [EMIM][N(CN)2], and [OMA][NTf2] in Dependence on Temperature at Atmospheric Pressure. *The Journal of Physical Chemistry B* **2008,** *112* (39), 12420-12430.
30. Eshelby, J. D.; Peierls, R. E., The Determination of the Elastic Field of an Ellipsoidal Inclusion, and Related Problems. *Proceedings of the Royal Society of London. Series A. Mathematical and Physical Sciences* **1957,** *241* (1226), 376-396.
31. Mancarella, F.; Style, R. W.; Wettlaufer, J. S., Surface Tension and The Mori-Tanaka Theory of Non-Dilute Soft Composite Solids. *Proceedings of the Royal Society A: Mathematical, Physical and Engineering Sciences* **2016,** *472* (2189), 20150853.
32. Style, R. W.; Boltyanskiy, R.; Allen, B.; Jensen, K. E.; Foote, H. P.; Wettlaufer, John S.; Dufresne, E. R., Stiffening Solids with Liquid Inclusions. *Nature Physics* **2014,** *11*, 82–87.
33. Carpi, F.; Anderson, I.; Bauer, S.; Frediani, G.; Gallone, G.; Gei, M.; Graaf, C.; Jean-Mistral, C.; Kaal, W.; Kofod, G.; Kollosche, M.; Kornbluh, R.; Lassen, B.; Matysek, M.; Michel, S.; Nowak, S.; O'Brien, B.; Pei, Q.; Pelrine, R.; Rechenbach, B.; Rosset, S.; Shea, H., Standards for Dielectric Elastomer Transducers. *Smart Materials and Structures* **2015,** *24* (10), 105025.
34. Aguilar Bolados, H.; Hernández-Santana, M.; Romasanta, L. J.; Yazdani-Pedram, M.; Quijada, R.; López-Manchado, M. A.; Verdejo, R., Electro-Mechanical Actuation Performance of SEBS/PU Blends. *Polymer* **2019,** *171*, 25-33.
35. Yang, D.; Ruan, M.; Huang, S.; Wu, Y.; Li, S.; Wang, H.; Shang, Y.; Li, B.; Guo, W.; Zhang, L., Improved Electromechanical Properties of NBR Dielectric Composites by Poly(dopamine) and Silane Surface Functionalized TiO2 Nanoparticles. *Journal of Materials Chemistry C* **2016,** *4* (33), 7724-7734.
36. Mazurek, P.; Hvilsted, S.; Skov, A. L., Green Silicone Elastomer Obtained from a Counterintuitively Stable Mixture of Glycerol and PDMS. *Polymer* **2016,** *87*, 1-7.
37. Mazurek, P.; Yu, L.; Gerhard, R.; Wirges, W.; Skov, A. L., Glycerol as High-Permittivity Liquid Filler in Dielectric Silicone Elastomers. *Journal of Applied Polymer Science* **2016,** *133* (43).
38. Pan, C.; Markvicka, E. J.; Malakooti, M. H.; Yan, J.; Hu, L.; Matyjaszewski, K.; Majidi, C., A Liquid-Metal–Elastomer Nanocomposite for Stretchable Dielectric Materials. *Advanced Materials* **2019,** *31* (23), 1900663.

39. Yuk, H.; Zhang, T.; Lin, S.; Parada, G. A.; Zhao, X., Tough Bonding of Hydrogels to Diverse Non-Porous Surfaces. *Nature Materials* **2015,** *15*, 190–196.
40. Phadke, A.; Zhang, C.; Arman, B.; Hsu, C.-C.; Mashelkar, R. A.; Lele, A. K.; Tauber, M. J.; Arya, G.; Varghese, S., Rapid Self-Healing Hydrogels. *Proceedings of the National Academy of Sciences* **2012,** *109* (12), 4383-4388.
41. Arikawa, H.; Kanie, T.; Fujii, K.; Takahashi, H.; Ban, S., Effect of Filler Properties in Composite Resins on Light Transmittance Characteristics and Color. *Dental Materials Journal* **2007,** *26* (1), 38-44.
42. Lee, S.; Reuveny, A.; Reeder, J.; Lee, S.; Jin, H.; Liu, Q.; Yokota, T.; Sekitani, T.; Isoyama, T.; Abe, Y.; Suo, Z.; Someya, T., A Transparent Bending-Insensitive Pressure Sensor. *Nature Nanotechnology* **2016,** *11* (5), 472-478.
43. Lipomi, D. J.; Vosgueritchian, M.; Tee, B. C. K.; Hellstrom, S. L.; Lee, J. A.; Fox, C. H.; Bao, Z., Skin-Like Pressure and Strain Sensors Based on Transparent Elastic Films of Carbon Nanotubes. *Nature Nanotechnology* **2011,** *6* (12), 788-792.
44. Kulkarni, M. R.; John, R. A.; Rajput, M.; Tiwari, N.; Yantara, N.; Nguyen, A. C.; Mathews, N., Transparent Flexible Multifunctional Nanostructured Architectures for Non-optical Readout, Proximity, and Pressure Sensing. *ACS Applied Materials & Interfaces* **2017,** *9* (17), 15015-15021.
45. Ruth, S. R. A.; Beker, L.; Tran, H.; Feig, V. R.; Matsuhisa, N.; Bao, Z., Rational Design of Capacitive Pressure Sensors Based on Pyramidal Microstructures for Specialized Monitoring of Biosignals. *Advanced Functional Materials 0* (0), 1903100.
46. Shi, H.; Al-Rubaiai, M.; Holbrook, C. M.; Miao, J.; Pinto, T.; Wang, C.; Tan, X., Screen-Printed Soft Capacitive Sensors for Spatial Mapping of Both Positive and Negative Pressures. *Advanced Functional Materials* **2019,** *29* (23), 1809116.
47. Franchi, M. V.; Reeves, N. D.; Narici, M. V., Skeletal Muscle Remodeling in Response to Eccentric vs. Concentric Loading: Morphological, Molecular, and Metabolic Adaptations. *Frontiers in Physiology* **2017,** *8* (447).
48. Niu, X.; Stoyanov, H.; Hu, W.; Leo, R.; Brochu, P.; Pei, Q., Synthesizing a New Dielectric Elastomer Exhibiting Large Actuation Strain and Suppressed Electromechanical Instability without Prestretching. *Journal of Polymer Science Part B: Polymer Physics* **2013,** *51* (3), 197-206.
49. Kellaris, N.; Gopaluni Venkata, V.; Smith, G. M.; Mitchell, S. K.; Keplinger, C., Peano-HASEL Actuators: Muscle-Mimetic, Electrohydraulic Transducers that Linearly Contract on Activation. *Science Robotics* **2018,** *3* (14), eaar3276.
50. Duduta, M.; Wood, R. J.; Clarke, D. R., Multilayer Dielectric Elastomers for Fast, Programmable Actuation without Prestretch. *Advanced Materials* **2016,** *28* (36), 8058-8063.
51. Shi, L.; Yang, R.; Lu, S.; Jia, K.; Xiao, C.; Lu, T.; Wang, T.; Wei, W.; Tan, H.; Ding, S., Dielectric Gels with Ultra-High Dielectric Constant, Low Elastic Modulus, and Excellent Transparency. *NPG Asia Materials* **2018,** *10* (8), 821-826.
52. John, R. A.; Tiwari, N.; Yaoyi, C.; Ankit; Tiwari, N.; Kulkarni, M.; Nirmal, A.; Nguyen, A. C.; Basu, A.; Mathews, N., Ultralow Power Dual-Gated Subthreshold Oxide Neuristors: An Enabler for Higher Order Neuronal Temporal Correlations. *ACS Nano* **2018,** *12* (11), 11263-11273.
53. Tiwari, N.; Ho, F.; Ankit; Mathews, N., A Rapid Low Temperature Self-Healable Polymeric Composite for Flexible Electronic Devices. *Journal of Materials Chemistry A* **2018,** *6* (43), 21428-21434.

TABLE OF CONTENT (TOC) FIGURE